

# Processing, microstructure and mechanical properties of $\text{Al}_2\text{O}_3$ –Cr nanocomposites

Chmielewski Marcin<sup>\*</sup>, Pietrzak Katarzyna

*Institute of Electronic Materials Technology, 133 Wolczynska Str, 01-919 Warsaw, Poland*

Available online 27 June 2006

## Abstract

Alumina–chromium composites are well known for their good mechanical properties in comparison with pure alumina or metals. The composites have high hardness, high mechanical strength and because of their strong resistance to abrupt changes of temperature within the 25–1300 °C range or high temperature resistance to oxidation, they can be used at temperatures exceeding 1000 °C. Most of earlier works tended to use particles in the micrometer range. In this work,  $\text{Al}_2\text{O}_3$ –Cr nanocomposites with 25, 50 and 75 vol.% Cr were made by pressureless sintering and hot pressing of aluminium oxide nanopowder (~80 nm) and chromium particles in the micrometer range. The presented paper concerns the examination of the microstructure and mechanical properties (hardness, bending strength, wear resistance) of  $\text{Al}_2\text{O}_3$ –Cr nanocomposites. The microstructural examinations (optical, scanning and transmission microscopy) show that almost fully dense materials can be obtained (typically 98–99% of theoretical density), when pressureless sintering at 1600 °C or hot pressing at 1400 °C. Moreover, the sintering process did not cause any major changes in the structure of the composite, although it was stated significant growth of the  $\text{Al}_2\text{O}_3$  nanograins.

© 2006 Elsevier Ltd. All rights reserved.

**Keywords:**  $\text{Al}_2\text{O}_3$ –Cr composites; Hot pressing; Mechanical properties

## 1. Introduction

The applications of alumina ceramics as structural components are often limited by its brittleness. The addition of second phase inclusions, especially metal phases, may help to overcome this drawback. A large number of metals have been added to alumina, including Ni, Mo, W, Fe, Cr and Cu.<sup>1</sup> Due to their good mechanical properties, alumina–chromium composites are widely used to make many constructional elements, e.g. parts of jet engines, tools, thermal screens, etc.,<sup>2</sup> characterised by a high hardness and mechanical strength, excellent oxidation resistance and chemical stability. Moreover, aluminium and chromium oxides have the same crystal structures and are completely soluble, what may help to achieve a good bonding between the metal and oxide phases.<sup>3</sup> Alumina–chromium composites have been obtained using pressureless sintering,<sup>1</sup> hot pressing<sup>4</sup> and combustion synthesis,<sup>5</sup> processed from different forms and grain sizes of powders, including nanopowders,<sup>6</sup> powders obtained by mechanical alloying and powders reaction milling of aluminium and chromium oxides ( $\text{CrO}_3$ ,  $\text{Cr}_2\text{O}_3$ ).<sup>4</sup>

The aim of this work was to obtain fully dense alumina–chromium composites using an aluminium oxide nanopowder, and to characterise the microstructure and mechanical properties of  $\text{Al}_2\text{O}_3$ –Cr composites with different amounts of metal phase.

## 2. Experimental procedure

In the present work the nanometer powder of aluminium oxide (China, average grain size 80 nm, Fig. 1) and the chromium powder (NewMet Koch, <40 µm, Fig. 2) were used. Three powder mixtures compositions with the following  $\text{Al}_2\text{O}_3$  to Cr ratio (in vol.%): 25 $\text{Al}_2\text{O}_3$ /75 Cr, 50 $\text{Al}_2\text{O}_3$ /50Cr and 75 $\text{Al}_2\text{O}_3$ /25Cr were prepared. The powder mixtures were dry-milled with the use of alumina milling balls (Ø = 8 mm).

Microstructural observations (Fig. 3) of the powder mixtures for different milling time revealed that a milling time below 4 h does not ensure a homogeneous powder mixture, and milling times beyond 12 h resulted in the growth of  $\text{Al}_2\text{O}_3$  agglomerates on the surface of chromium powder. The tests showed that the optimal milling time to obtain homogeneous powder mixtures without vast quantities of aluminium oxide powder agglomerates was 8 h.

<sup>\*</sup> Corresponding author.

E-mail address: [chmiel-m@sp.itme.edu.pl](mailto:chmiel-m@sp.itme.edu.pl) (M. Chmielewski).

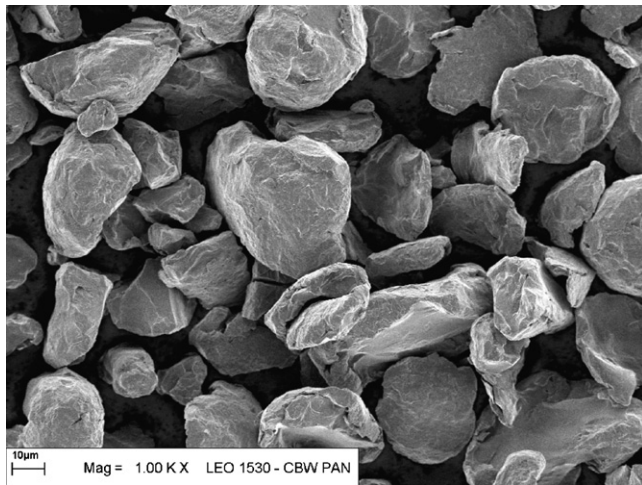


Fig. 1. Microstructure of the chromium starting powder.

$\text{Al}_2\text{O}_3$ –Cr pellets were formed by uniaxial pressing in a 30 mm diameter cylindrical steel die with a pressure of 0.2 MPa and isostatically pressed at 120 MPa.

Prepared samples were pressureless sintered (PS) and hot pressed (HP). The sintering process was performed in vacuum ( $1.3 \times 10^{-3}$  Pa), in the 1400–1600 °C range. Hot pressing was performed in a Thermal Technology Astro press in argon atmosphere using a graphite mould at 1200–1400 °C. A pressure of 30 MPa was applied after reaching the sintering temperature. The heating rate was 10 °C/min and the samples were cooled naturally to room temperature. Pressureless sintering and hot pressing was performed with a dwell time of 60 min.

Microstructural investigations included optical microscopy (Olympus SZX9), scanning electron microscopy (SEM, Hitachi S4100 and Opton DSM 950) and transmission electron microscopy (TEM, Hitachi H9000-NA). The samples were mechanical cut, ground and polished. For SEM observations the samples were covered with a thin layer of carbon. The TEM samples were additionally polished and ion-beam etched (Baltec Rapid System).

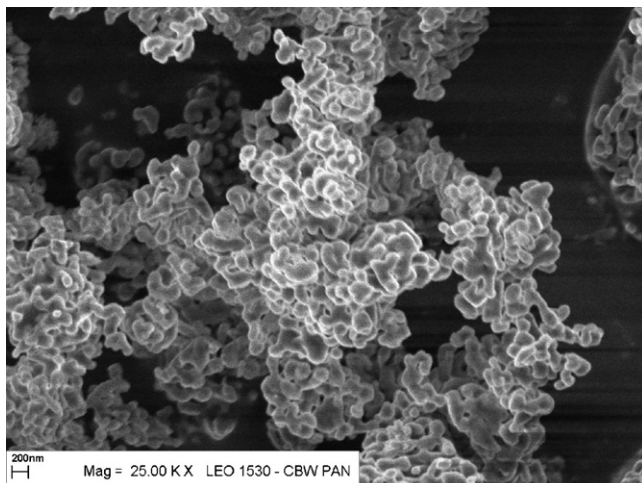


Fig. 2. Microstructure of the aluminium oxide nanopowder.

The density of the  $\text{Al}_2\text{O}_3$ –Cr composites was measured according to the Archimedes method. The hardness (HV10) was tested with a Vickers diamond indenter using a load of 98 N with loading time of 10 s. Each indentation was placed at least 10 diagonal lengths away from adjacent indentation. The hardness results were averaged over 10 indentations per specimens. The flexure strength measurements of the obtained  $\text{Al}_2\text{O}_3$ –Cr composites were performed using a Zwick 1446 testing machine for a sample dimension of 2 mm × 3 mm × 25 mm. The three-point bending mode measurements were made with a span of 20 mm and a displacement rate of 1 mm/min. Average values of the bending strength were calculated from five tests. The wear resis-

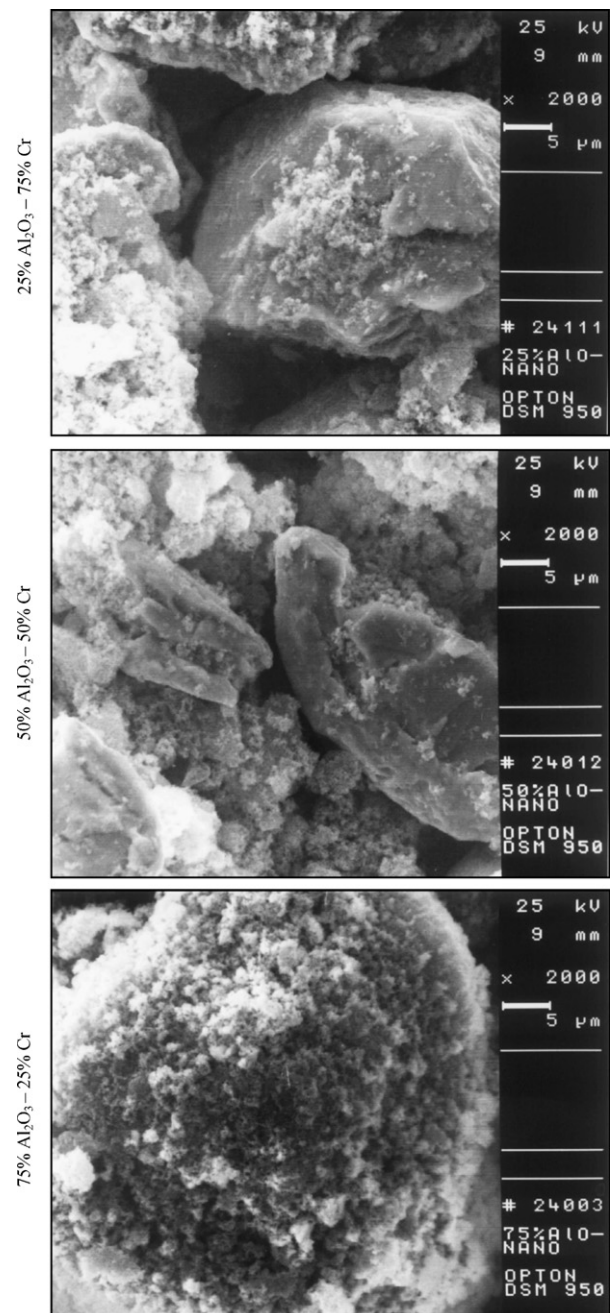


Fig. 3. SEM micrographs of the  $\text{Al}_2\text{O}_3$ –Cr powder mixtures (milling time 8 h): (a) 25%  $\text{Al}_2\text{O}_3$ –75%Cr, (b) 50%  $\text{Al}_2\text{O}_3$ –50%Cr and (c) 75%  $\text{Al}_2\text{O}_3$ –25%Cr.

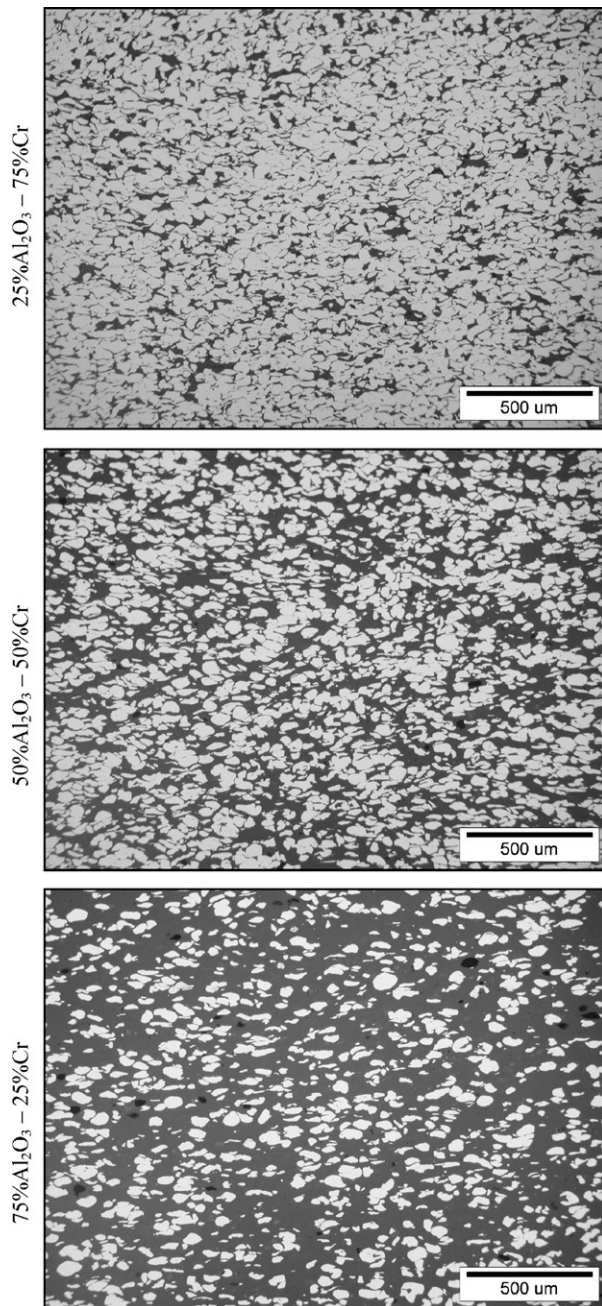


Fig. 4. Microstructure of hot pressed ( $T=1400^{\circ}\text{C}$ ,  $p=30\text{ MPa}$ ,  $t=60\text{ min}$ )  $\text{Al}_2\text{O}_3$ –Cr composites with different amounts of metal phase: (a)  $25\%\text{Al}_2\text{O}_3$ – $75\%\text{Cr}$ , (b)  $50\%\text{Al}_2\text{O}_3$ – $50\%\text{Cr}$  and (c)  $75\%\text{Al}_2\text{O}_3$ – $25\%\text{Cr}$ .

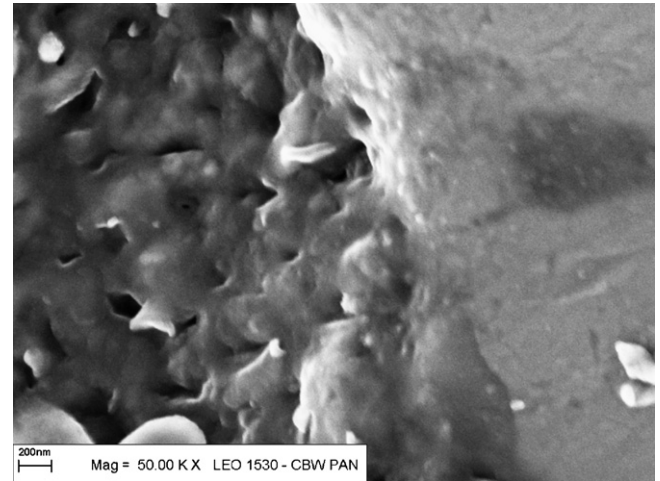


Fig. 5. Scanning electron micrograph of the chromium-alumina border in the  $75\text{Al}_2\text{O}_3/25\text{Cr}$  nanocomposite.

tance test the surface of polished was tested against a sapphire ball ( $\varnothing=5\text{ mm}$ ) counterbody. The conditions of the reciprocative sliding test were: a load  $50\text{ N}$ , time  $30\text{ min}$ , frequency  $1\text{ Hz}$ , amplitude  $4.5\text{ mm}$ , temperature  $24^{\circ}\text{C}$  and humidity  $75\%$ . After the test, the wear track was measured using a Form Talysurf Series 2 profilometer.

### 3. Results and discussion

The theoretical densities of the composites were calculated assuming a density of aluminium oxide  $\rho_{\text{Al}_2\text{O}_3} = 3.97\text{ g/cm}^3$  and chromium  $\rho_{\text{Cr}} = 7.19\text{ g/cm}^3$ , resulting in for the composition  $25\text{Al}_2\text{O}_3/75\text{Cr}$ — $\rho_{\text{T}} = 6.385\text{ g/cm}^3$ , for the composition  $50\text{Al}_2\text{O}_3/50\text{Cr}$ — $\rho_{\text{T}} = 5.58\text{ g/cm}^3$  and for the composition  $75\text{Al}_2\text{O}_3/25\text{Cr}$ — $\rho_{\text{T}} = 4.775\text{ g/cm}^3$ , respectively. The densities of the  $\text{Al}_2\text{O}_3$ –Cr composites obtained by pressureless sintering and hot pressing are presented in Tables 1 and 2, respectively.

The density tests confirmed the possibility of obtaining nearly theoretically dense  $\text{Al}_2\text{O}_3$ –Cr composites of all powder compositions by both techniques (sintering and pressing). The hot pressing method however allowed obtaining the fully dense materials at a temperature of  $200^{\circ}\text{C}$  lower than in the case of pressureless sintering. The difference in the relative densities for different compositions was not significant, oscillating around  $1$ – $2\%$ .

The microstructures of the  $\text{Al}_2\text{O}_3$ –Cr composites obtained by the hot pressing are presented in Fig. 4, confirming the high

Table 1  
Density ( $\rho$ ) and relative density ( $S$ ) of pressureless sintered  $\text{Al}_2\text{O}_3$ –Cr composites

Composition (vol.%)	Temperature ( $^{\circ}\text{C}$ )					
	1400		1500		1600	
	$\rho\text{ (g/mm}^3\text{)}$	$S\text{ (}\%\text{)}$	$\rho\text{ (g/mm}^3\text{)}$	$S\text{ (}\%\text{)}$	$\rho\text{ (g/mm}^3\text{)}$	$S\text{ (}\%\text{)}$
$25\%\text{Al}_2\text{O}_3$ – $75\%\text{Cr}$	5.49	86.0	5.98	93.6	6.32	99.0
$50\%\text{Al}_2\text{O}_3$ – $50\%\text{Cr}$	4.73	84.8	5.18	92.8	5.47	98.0
$75\%\text{Al}_2\text{O}_3$ – $25\%\text{Cr}$	4.02	84.2	4.39	91.9	4.64	97.2



Table 2  
Density ( $\rho$ ) and relative density ( $S$ ) of hot pressed  $\text{Al}_2\text{O}_3\text{--Cr}$  composites

Composition (vol.%)	Temperature ( $^{\circ}\text{C}$ )									
	1200		1250		1300		1350		1400	
	$\rho$ (g/mm $^3$ )	$S$ (%)	$\rho$ (g/mm $^3$ )	$S$ (%)	$\rho$ (g/mm $^3$ )	$S$ (%)	$\rho$ (g/mm $^3$ )	$S$ (%)	$\rho$ (g/mm $^3$ )	$S$ (%)
25% $\text{Al}_2\text{O}_3\text{--}75\%\text{Cr}$	5.53	86.6	5.81	91.0	6.06	94.9	6.23	97.6	6.35	99.4
50% $\text{Al}_2\text{O}_3\text{--}50\%\text{Cr}$	4.82	86.4	5.04	90.3	5.20	93.2	5.39	96.6	5.52	98.9
75% $\text{Al}_2\text{O}_3\text{--}25\%\text{Cr}$	4.21	86.1	4.34	90.9	4.48	93.9	4.61	96.5	4.70	98.4

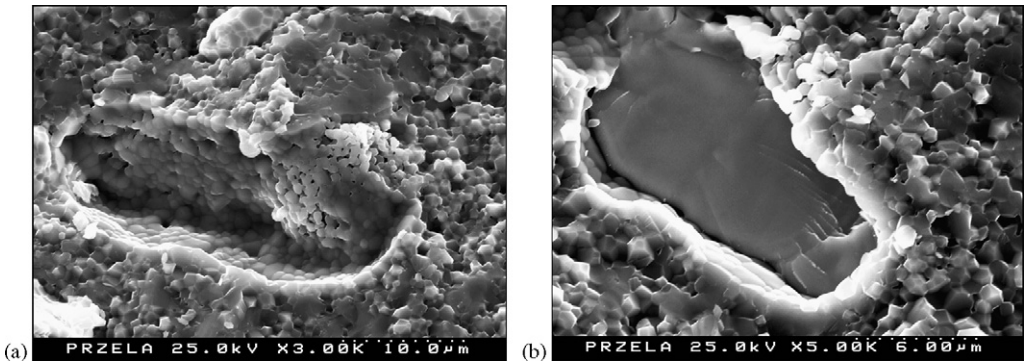


Fig. 6. The fracture surface of hot pressed  $\text{Al}_2\text{O}_3\text{--Cr}$  nanocomposite: intergranular fracture of the alumina nanograins (a) and transgranular fracture of a chromium grain (b).

densities of hot pressed  $\text{Al}_2\text{O}_3\text{--Cr}$  composites. Some remaining porosity, especially in the 75 $\text{Al}_2\text{O}_3$ /25Cr composites can be observed. However, all microstructures are characterised by a very good homogeneity. Some chromium particles, bright on

the micrographs, are slightly elongated in the direction perpendicular to the hot pressing direction.

Fig. 5 shows the microstructure at the border of a chromium grain in contact with  $\text{Al}_2\text{O}_3$  nanograins, hot pressed at 1400  $^{\circ}\text{C}$ .

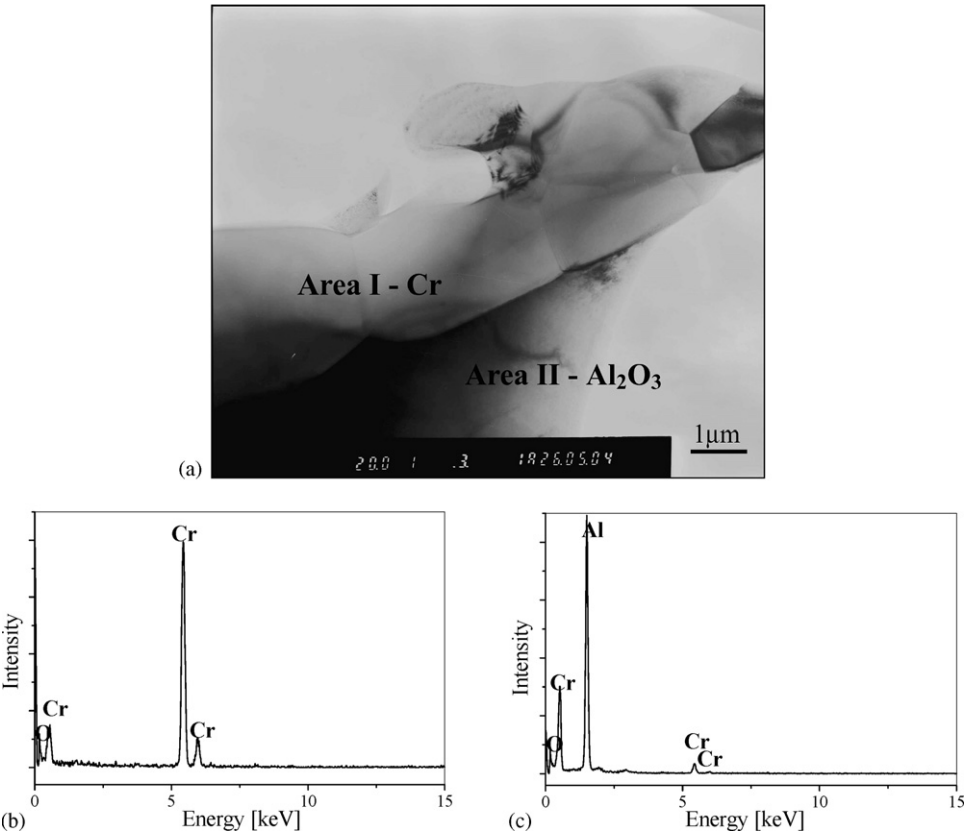


Fig. 7. TEM micrographs of the  $\text{Al}_2\text{O}_3\text{--Cr}$  nanocomposite (a) and EDS point analysis of area I (b) and area II (c).

Table 3

Mechanical properties of hot pressed ( $T = 1400^\circ\text{C}$ ,  $p = 30\text{ MPa}$ ,  $t = 60\text{ min}$ ) and pressureless sintered ( $T = 1600^\circ\text{C}$ ,  $t = 60\text{ min}$ )  $\text{Al}_2\text{O}_3\text{--Cr}$  composites

Composition (vol.%)	Sintering conditions	Density ( $\text{g/cm}^3$ )	Hardness (GPa)	Bending strength (MPa)
25% $\text{Al}_2\text{O}_3\text{--}75\%\text{Cr}$	PS $1600^\circ\text{C}/1\text{ h}$	6.32	$2.57 \pm 0.12$	$362.3 \pm 20.4$
	HP $1400^\circ\text{C}/1\text{ h}$	6.35	$2.81 \pm 0.11$	$392.3 \pm 13.9$
50% $\text{Al}_2\text{O}_3\text{--}50\%\text{Cr}$	PS $1600^\circ\text{C}/1\text{ h}$	5.47	$4.85 \pm 0.32$	$313.5 \pm 11.8$
	HP $1400^\circ\text{C}/1\text{ h}$	5.52	$5.30 \pm 0.25$	$349.9 \pm 4.2$
75% $\text{Al}_2\text{O}_3\text{--}25\%\text{Cr}$	PS $1600^\circ\text{C}/1\text{ h}$	4.64	$8.78 \pm 0.47$	$277.5 \pm 10.8$
	HP $1400^\circ\text{C}/1\text{ h}$	4.70	$9.51 \pm 0.34$	$314.8 \pm 9.5$

This analysis showed that the sintering process did not cause any major changes in the structure of the composite, although it was stated significant growth of the  $\text{Al}_2\text{O}_3$  nanograins. The average size of the  $\text{Al}_2\text{O}_3$  nanograins after hot pressing can be estimated at the 200–300 nm level and at the 500 nm level, in the case of pressureless sintering. There was not found

the effect of the Cr content on the  $\text{Al}_2\text{O}_3$  grain size. The growth of the nanograins could be caused by the long time of sintering (1 h). The attempts of the dwell time shortening to 0.5 h caused the raise of the porosity amount in  $\text{Al}_2\text{O}_3\text{--Cr}$  composites, especially close to the outside surface of the samples.

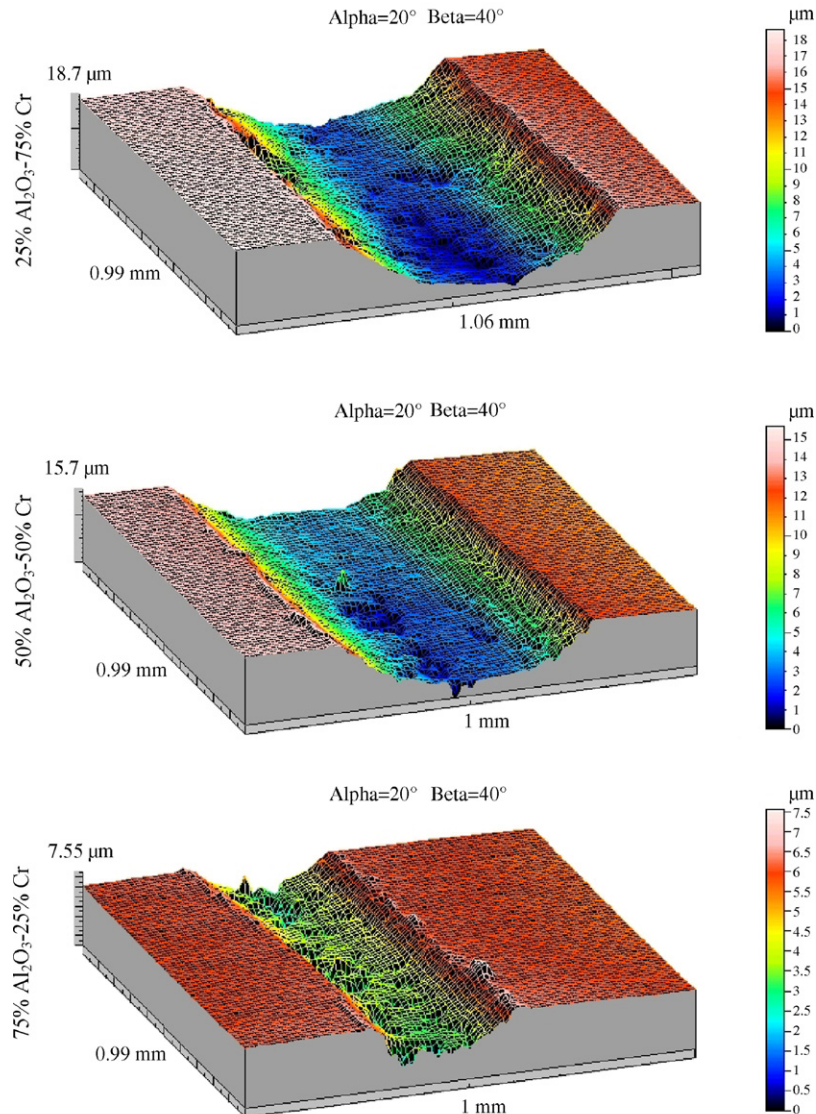


Fig. 8. Wear profiles on the different hot pressed  $\text{Al}_2\text{O}_3\text{--Cr}$  nanocomposites: (a) 25%  $\text{Al}_2\text{O}_3\text{--}75\%\text{Cr}$ , (b) 50%  $\text{Al}_2\text{O}_3\text{--}50\%\text{Cr}$  and (c) 75%  $\text{Al}_2\text{O}_3\text{--}25\%\text{Cr}$ .

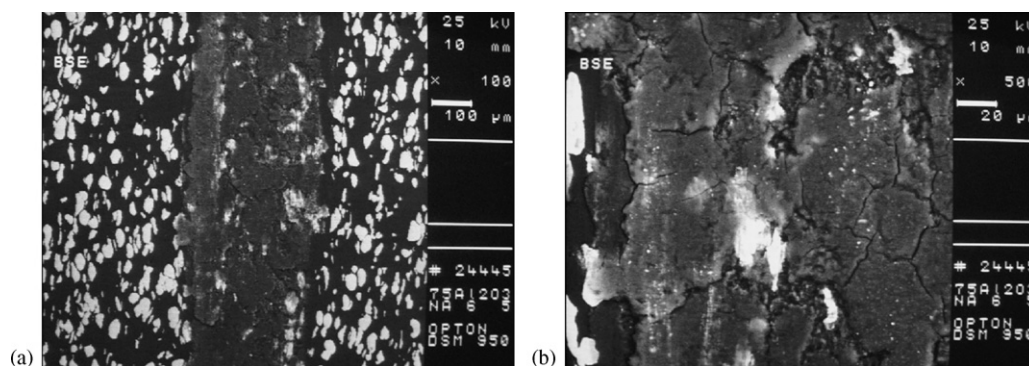


Fig. 9. (a and b) SEM micrographs of the wear track on the 75Al<sub>2</sub>O<sub>3</sub>/25Cr nanocomposite.

The X-ray phase analysis showed the presence of chromium and alumina phases. Only the surface of the hot pressed and pressureless sintered material contained small amounts of chromium carbide as a result of reaction with a graphite.

The SEM investigations of fracture surfaces of pressureless sintered and hot pressed composites (Fig. 6) revealed an intergranular fracture of the alumina grains and transgranular fracture of the chromium particles.

In the literature there are many hypotheses about the sintering mechanism in Al<sub>2</sub>O<sub>3</sub>–Cr composites, such as sintering with a Cr<sub>2</sub>O<sub>3</sub> interlayer.<sup>7</sup> Scanning microscopy analyses however did not allow to confirm the presence of such an interlayer. Transmission electron microscopy results are shown in Fig. 7, indicating the diffusion of chromium atoms into the alumina during sintering. Diffusion in the opposite way from alumina to chromium was not observed.

The hardness and bending strength of the Al<sub>2</sub>O<sub>3</sub>–Cr composites obtained by pressureless sintering ( $T = 1600^\circ\text{C}$ ) and hot pressing ( $T = 1400^\circ\text{C}$ ) are summarized in Table 3. These conditions were chosen for comparison due to the similar relative densities of the samples.

A significant differences in both hardness ( $\sim 10\%$ ) and in bending strength (10–15%) was observed for the sintering process. These differences can be attributed to the higher porosity and bigger alumina grain size in the case of pressureless sintered composites. The hardness is rising with increasing ceramic phase content, from 2.8 and 2.5 GPa for the 25Al<sub>2</sub>O<sub>3</sub>/75Cr composition, to 9.5 and 8.8 GPa for the 75Al<sub>2</sub>O<sub>3</sub>/25Cr composition, hot pressed and pressureless sintered, respectively. The hardness results correspond well with the results of composite densities. The bending strength also depends on the composition, technological conditions and sintering process. The bending strength decreases with increasing alumina phase content, due to increased brittle ceramic phase content. A maximum strength of  $\sim 400$  MPa was obtained for the 25Al<sub>2</sub>O<sub>3</sub>/75Cr composite.

Table 4  
The volumes of the groove after the resistance test

Composition (vol.%)	Volume ( $\times 10^6 \mu\text{m}^3$ )
25%Al <sub>2</sub> O <sub>3</sub> –75%Cr	5.30
50%Al <sub>2</sub> O <sub>3</sub> –50%Cr	3.71
75%Al <sub>2</sub> O <sub>3</sub> –25%Cr	0.50

The volumetric wear resistance along 1 mm length of the groove of hot pressed Al<sub>2</sub>O<sub>3</sub>–Cr nanocomposites is summarised in Table 4.

The wear resistance increased with increasing Al<sub>2</sub>O<sub>3</sub> content in the composite, as shown in Fig. 8, presenting the wear profiles on different hot pressed Al<sub>2</sub>O<sub>3</sub>–Cr nanocomposites. There are visible the differences in the width and depth of the groove. The microstructure of the 75Al<sub>2</sub>O<sub>3</sub>/25Cr nanocomposite wear track test shown in Fig. 9, reveals the presence of cracked adhering wear debris forming an interlayer between the contacting bodies.

#### 4. Conclusions

Based on these studies it can be concluded that:

- Hot pressing at  $1400^\circ\text{C}$  allowed obtaining near fully dense Al<sub>2</sub>O<sub>3</sub>–Cr nanocomposites at a temperature of  $200^\circ\text{C}$  lower than in the case of pressureless sintering.
- For the investigated composites with 25, 50 and 75 vol.% Cr, the hardness and bending strength were higher for hot pressed Al<sub>2</sub>O<sub>3</sub>–Cr nanocomposites compared to pressureless sintered grades, due to the finer Al<sub>2</sub>O<sub>3</sub> grains size and lower porosity level after hot pressing.
- The increase of the ceramics grains' size was lower for hot pressing method (average grain size  $\sim 200$  nm) than in the case of pressureless sintering method (average grain size  $\sim 500$  nm).
- TEM investigation of hot pressed Al<sub>2</sub>O<sub>3</sub>–Cr nanocomposites showed the diffusion of chromium atoms into the Al<sub>2</sub>O<sub>3</sub> grains,
- Properties of Al<sub>2</sub>O<sub>3</sub>–Cr composites depend on applied sintering method and process conditions; the hardness and the wear resistance of hot pressed and pressureless sintered Al<sub>2</sub>O<sub>3</sub>–Cr composites are rising with increasing ceramic phase content; the bending strength decreases with increasing alumina phase content.

#### Acknowledgement

The authors would like to thank the Polish State Committee for Scientific Research for the financial support under Project No. 3T08A 080 27.

## References

1. Ji, Y. and Yeomans, J. A., Microstructure and mechanical properties of chromium and chromium/nickel particulate reinforced alumina ceramics. *J. Mater. Sci.*, 2002, **37**, 5229–5236.
2. Włosiński, W., Al<sub>2</sub>O<sub>3</sub>–Cu and Al<sub>2</sub>O<sub>3</sub>–Cr composite technology and properties, sintered metal–ceramic composite. *Materials Science Monographs* 25. G.S. Upadhyaya, Amsterdam, 1984.
3. Hirata, T., Akiyama, K. and Yamamoto, H., Sintering behavior of Cr<sub>2</sub>O<sub>3</sub>–Al<sub>2</sub>O<sub>3</sub> ceramics. *J. Eur. Ceram. Soc.*, 2000, **20**, 195–199.
4. Guichard, J. L., Tillement, O. and Mocellin, A., Alumina–chromium cermets by hot-pressing of nanocomposite powders. *J. Eur. Ceram. Soc.*, 1998, **18**, 1743–1752.
5. Zeng, X., Sun, G. and Zhang, S., Combustion synthesis of Al<sub>2</sub>O<sub>3</sub>(–Cr<sub>2</sub>O<sub>3</sub>)–Cr cermets. *Scripta Mater.*, 2000, **42**, s.1167–s.1172.
6. Ji, Y. and Yeomans, J. A., Processing and mechanical properties of Al<sub>2</sub>O<sub>3</sub>–5 vol.% Cr nanocomposites. *J. Eur. Ceram. Soc.*, 2002, **22**, s.1927–s.1936.
7. Bukat, A. and Rutkowski, W., *Theoretical Basis of Sintering Processes*. Silesian Edition, 1974.